

# DESIGN AND EVALUATION OF THE LOW-LEVEL RF ELECTRONICS FOR THE ILC MAIN LINAC\*

U. Mavric<sup>#</sup>, B. Chase, J. Branlard, V. Tupikov, B. Barnes, D. Klepec, Fermilab, Batavia, IL 60510

## Abstract

The proposed 30 km long ILC electron/positron collider is pushing the limits not only in basic physics research but also in engineering. For the two main LINACs, the pulsed RF power that is feeding the high number of SC RF cavities (~ 17 000) must be regulated to app. 0.1% for amplitude and 0.2° for phase. This guarantees the required energy spread (0.1%) at the interaction point in the detector. The regulation of phase and amplitude is carried out by the analog/digital electronics also denoted as the low-level RF control system. Besides meeting the regulation specifications, the low-level RF must be reliable, robust and low cost. In the paper we present a possible hardware solution that addresses these issues. The system is evaluated on a cavity emulator implemented on the FPGA. We also present measurement carried out at AØ photo injector.

## INTRODUCTION

The two main LINACs for the proposed ILC, will accelerate electrons and positron from 15 MeV up to 250 GeV with the goal luminosity of  $2 \cdot 10^{34} \text{ cm}^{-2} \text{ s}^{-1}$ . The energy spread of the beam, introduced by the RF system will be mitigated by the low-level RF (LLRF) control system. The lowest achievable energy spread is ultimately defined by the disturbances introduced by the electronics that is controlling it. Besides regulation requirements, the LLRF electronics for the ILC main LINACs must address also reliability, price, low power consumption, mechanical robustness and ease of automation. It is worth noting that the LLRF will have to process over 50 000 RF channels (pick-up probes, reference signals, reflected power, forward power, beam signals, interlocks etc.) coming from both LINACs.

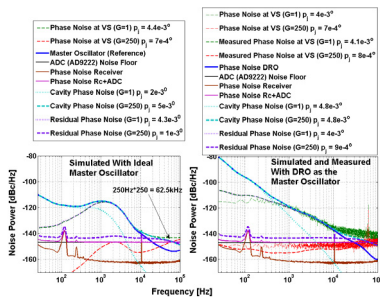


Figure 1: Analysis of close-in noise at various loop gains (>250). The analysis is done at the vector sum, at the output of the cavity and as a relative measurement of the beam compared to the cavity phase uncertainty.

## Regulation Requirements

According to [1], the correlated error at the interaction point should be lower than 0.5% for amplitude and 0.24° for phase. The unanswered question at this point is what is the allowed contribution of the LLRF system to this error budget? Ultimately, the measurement of the residual phase (meaning the relative fluctuation of beam compared to the cavity field) is limited by the noise added in the receiver. After various measurements on-the-bench we proved that a 12 bit (-147dBc/Hz noise floor, AD9222) ADC meets the regulation requirements for the ILC main LINACs. Fig.1 shows a theoretical analysis of the expected regulation at very high gains.

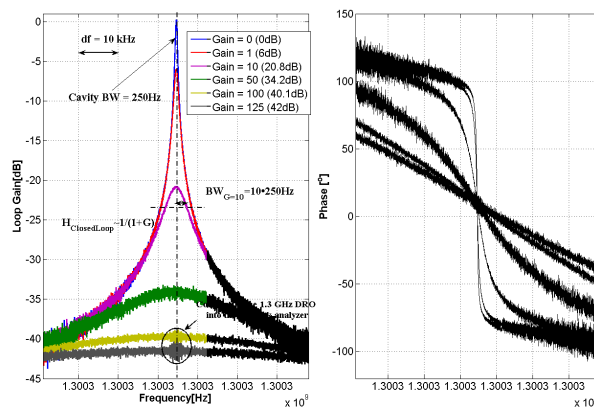


Figure 2: Transfer function of disturbance injected before the cavity to the output of the cavity.

Further on we will present the practical implementation of the LLRF and the evaluation of the system by using a cavity simulator and on an operating machine (AØ photo injector at Fermilab).

## THE LLRF SYSTEM FOR THE ILC MAIN LINACs

The system presented in this paper is composed of the 33 channel digital board (Multichannel Field Controller - MFC) and the nine channel analog receiver/transmitter board. The 1.3GHz RF signal is first downconverted by mixing with the LO at 1.313GHz to get the IF at 13MHz. The LO is generated in a separate chassis. The processing of the signal in digital domain is shown in Fig.3. The analog downconversion is done by using the 8 channel receiver/transmitter presented in [2].

\*Work supported by ...  
<sup>#</sup> mavric@fnal.gov

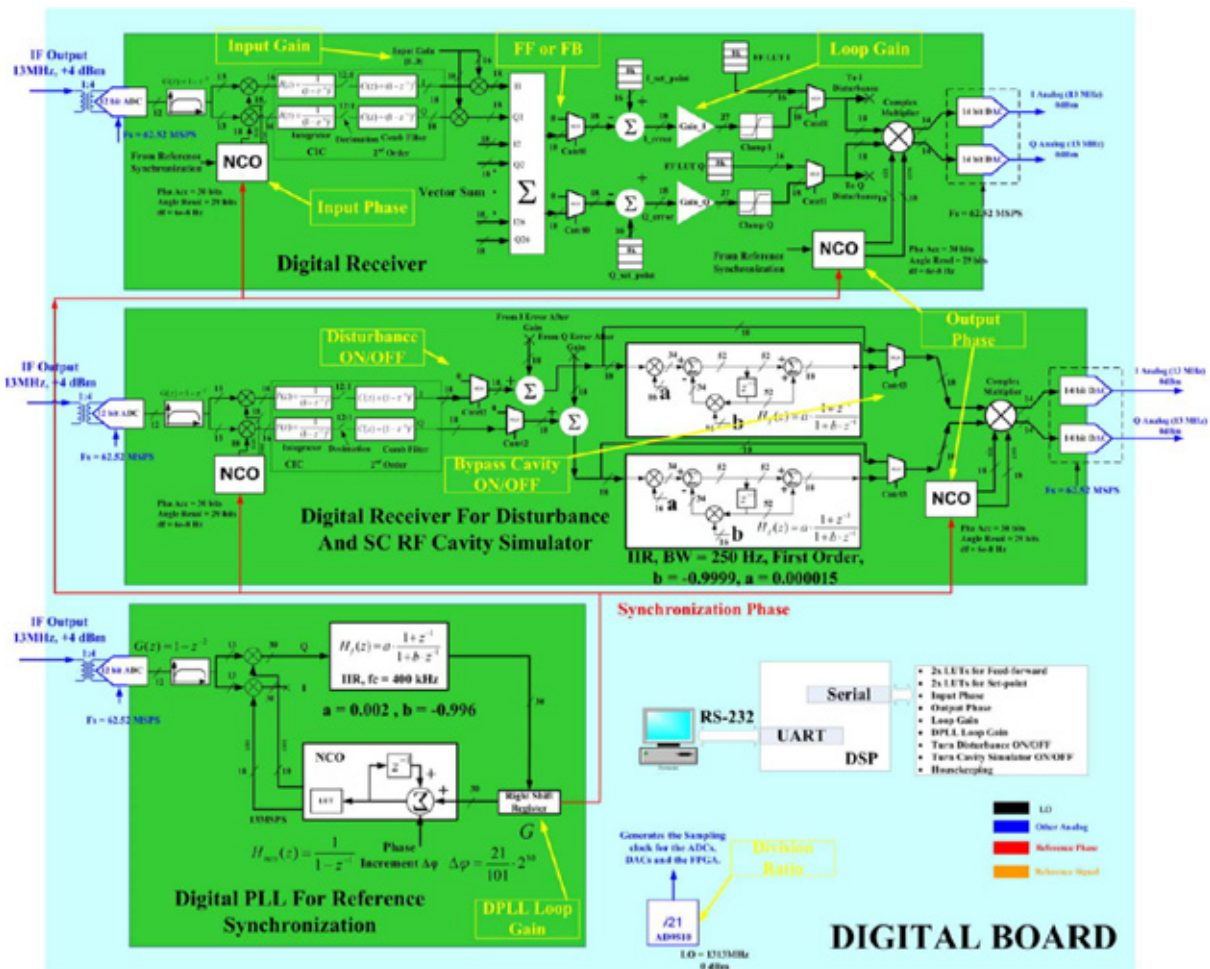


Figure 2: Block diagram of the firmware implemented on the FPGA. The main building blocks are the digital downconverter, the digital PLL synchronization with the reference, the digital upconverter, the controller, the cavity simulator and the disturbance channel.

### ON-THE-BENCH MEASUREMENTS

We simulated the superconducting (SC) cavity with a narrowband (half bandwidth 250Hz) IIR filter. An additional RF input allowed us to inject an arbitrary disturbance. By using the disturbance channel we also measured the transfer function of the disturbance to the output of the cavity as shown in Fig.3.

### MEASUREMENTS AT AØ PHOTO INJECTOR

We used the presented LLRF system to control capture cavity I, which is a 9-cell SC RF cavity with half bandwidth close to 100Hz and loaded QL ~ 6·10<sup>6</sup>. Fig.4 shows the transient at the flat-top after perturbing the closed loop with an impulse superimposed on the feed-forward drive signal. We managed to increase the loop gains up to 1000 (closed loop bandwidth close to 100 kHz) before noticeable instabilities could be seen. The first instabilities we noticed were caused by the 8π/9 mode.

### Phase and Amplitude Uncertainty

Fig.5 shows amplitude (in %) and phase (in °) uncertainty as function of loop gain. The minimum amplitude and phase standard deviations we are able to achieve is 0.016% and 0.016 ° over 1 MHz bandwidth. Calculations of the theoretical limitations (-147dBc/Hz over the same bandwidth) of the ADC give integrated uncertainty 0.0044% and 0.0026°. However, the phase noise before the subtraction in the feedback loop is twice the residual phase noise generated by the receiver. The reason lays in the reference receiver, which synchronizes the 1.3GHz reference signal and applies a phase correction to all the down and up converters in the design. Consequently, there is approximately a factor of ~3.6 for the amplitude and a factor of ~3 for phase discrepancy between the measured and calculated values.

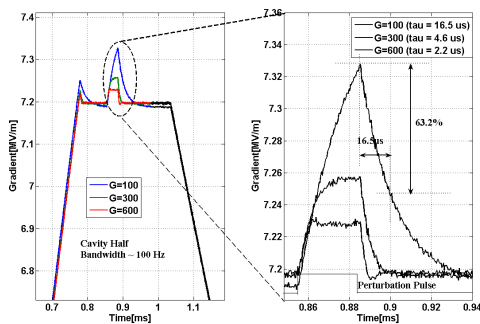


Figure 4: Response of the system measured before the subtraction after an impulse perturbation of the closed loop. Out of the exponential characteristic one can calculate the loop gain (half bandwidth is \$100Hz\$).

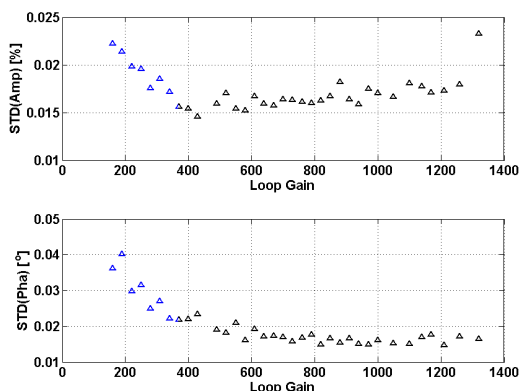


Figure 5: Amplitude and phase uncertainty measured before the subtraction as a function of loop gain. At gain larger than 1000 the system becomes unstable.

*Energy Dispersion Measurements*

Measurements of the energy spread were done by using a spectrometer. A bending magnet steers the particle by an angle, which depends on the energy of the particle. The beam position monitor located after the bending magnet detects the horizontal and vertical position of the beam. This information can be used to calculate the energy spread of the beam. Fig.7 shows the energy spread as a function of the loop gain. We repeated the measurements at different phase locations of the accelerating curve. Acceleration at 5 ° off-crest is less susceptible to phase deviations than at 26 ° off-crest acceleration.

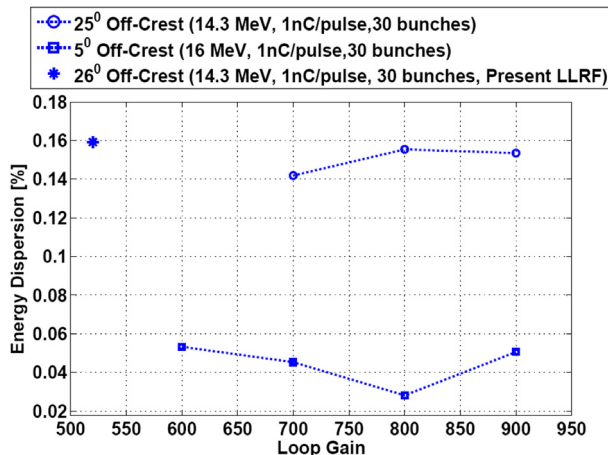


Figure 7: Energy spread measurements at A0 on CCI using a spectrometer. The present LLRF system is achieving twice that good performance at loop gain close to 520. However it is not capable of larger closed loop bandwidths due to the instabilities.

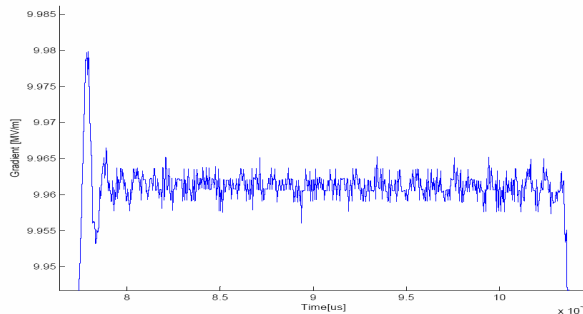


Figure 6: Regulation of flat-top region at loop gain of 970.

**CONCLUSIONS**

The presented LLRF system is a cost effective solution for RF systems where a large number of channels needs to be processed. At the same time the performance meet the ILC main LINACs specifications. In the future we intend to do more research on the factor of 3 discrepancies between the measured and expected regulation uncertainty. Also, we believe there is a significant contribution of the energy spread of the beam coming from the sections that proceed (RF gun, laser etc.) the cavity we are controlling.

**REFERENCES**

[1] Global Design Effort, "International Linear Collider Reference Design Report - Volume 3" August 2007; <http://www.linearcollider.org/cms/?pid=1000437>.  
 [2] U. Mavric, B. Chase and M. Vidmar., "Design and evaluation of a low-level RF control system analog/digital receiver for the ILC main LINACs", Nuclear Instruments & Methods in Physics Research Section A, August 2008, vol. 594, no. 1, pp. 90-96.